1310 *Biochemistry* **2010,** *49,* 1310–1318
DOI: 10.1021/bi9015499

BIOCHEMISTRY
including biophysical chemistry & molecular biology
Article

Hydrogen Bonding Progressively Strengthens upon Transfer of the Protein Urea-Denatured State to Water and Protecting Osmolytes[†]

Luis Marcelo F. Holthauzen, Jörg Rösgen,*[,‡] and D. Wayne Bolen*

Department of Biochemistry and Molecular Biology, University of Texas Medical Branch, Galveston, Texas 77555-1052
[‡]Present address: Department of Biochemistry and Molecular Biology, Penn State College of Medicine, Hershey, PA 17033-0850

Received September 4, 2009; Revised Manuscript Received November 25, 2009

ABSTRACT: Using osmolyte cosolvents, we show that hydrogen-bonding contributions can be separated from hydrophobic interactions in the denatured state ensemble (DSE). Specifically, the effects of urea and the protecting osmolytes sarcosine and TMAO are reported on the thermally unfolded DSE of Nank4−7*, a truncated notch ankyrin protein. The high thermal energy of this state in the presence and absence of 6 M urea or 1 M sarcosine solution is sufficient to allow large changes in the hydrodynamic radius (R_h) and secondary structure accretion without populating the native state. The CD change at 228 nm is proportional to the inverse of the volume of the DSE, giving a compact species equivalent to a premolten globule in 1 M sarcosine. The same general effects portraying hierarchical folding observed in the DSE at 55 °C are also often seen at room temperature. Analysis of Nank4−7* DSE structural energetics at room temperature as a function of solvent provides rationale for understanding the structural and dimensional effects in terms of how modulation of the solvent alters solvent quality for the peptide backbone. Results show that while the strength of hydrophobic interactions changes little on transferring the DSE from 6 M urea to water and then to 1 M TMAO, backbone−backbone (hydrogen-bonding) interactions are greatly enhanced due to progressively poorer solvent quality for the peptide backbone. Thus, increased intrachain hydrogen bonding guides secondary structure accretion and DSE contraction as solvent quality is decreased. This process is accompanied by increasing hydrophobic contacts as chain contraction gathers hydrophobes into proximity and the declining urea−backbone free energy gradient reaches urea concentrations that are energetically insufficient to keep hydrophobes apart in the DSE.

The relative importance and roles of hydrogen bonding and hydrophobic interactions in protein folding and stability is, arguably, one of the most contentious issues in protein folding (*1*). Because organic osmolytes affect hydrogen-bonding and hydrophobic interactions differentially (*1*−*3*), these physiologically important small molecules can be exploited to better understand the thermodynamics of protein folding/unfolding and stability. Here, we illustrate how knowledge of the energetic effects of osmolytes on the structure of the denatured state ensemble (DSE)[1] provides insight into the driving forces for solvent-mediated protein folding.

Numerous organisms use small organic osmolytes to offset protein denaturing conditions brought on by the environment (*4*, *5*). Given their important positions in biology, these molecules add new dimensions and viewpoints to studies of protein folding (*1*−*3*, *6*−*12*). The broad scope of osmolyte effects on protein folding ranges from the denaturing action of the physiologically important osmolyte, urea, to the exceptional ability of the protecting osmolytes, sarcosine and trimethylamine *N*-oxide (TMAO), in forcing proteins to fold (*13*−*16*). Understanding the impact of solvent components on proteins involves quantifying the changes they cause in the structure and dynamics of both native and denatured ensembles and identifying the underlying forces responsible. The native state structure is not noticeably perturbed by osmolytes, but the denatured state ensemble (DSE) exhibits plasticity evident in the changes in the DSE hydrodynamic radius (R_h) as a function of osmolyte type and concentration (*17*). In fact, an array of solvent effects on the contraction/expansion of the DSE has been described and sometimes associated with varying degrees of secondary and/or tertiary structure accretion (*17*−*22*). Notably, Uversky and Fink find strong correlation between the hydrodynamic volume of precursors of the native state and their degree of secondary structure, a correlation we extend to species that populate cosolvent-induced contraction of the DSE (*23*).

Owing to its dynamical and transient nature during folding, one of the effects most difficult to study involves contraction of the DSE to the point of collapse. This effect is observed in proteins that exhibit folding kinetics for which an initial rapid collapse of the DSE is followed by a rate-determining step leading to the native protein. Many of the mechanistic issues in folding kinetics involve limited subpopulations within the DSE such as those that promote nucleation and/or a coalescence of nonpolar side chains. The thermodynamics of native to denatured transitions, on the other hand, is inclusive in that it must account for the total population and thermodynamic character of the DSE

[†]Research was supported by NIH Grant GM49760.
*Corresponding authors. J.R.: e-mail, jur19@psu.edu; phone, 717-531-2026; fax, 717-531-7072. D.W.B.: e-mail, dwbolen@utmb.edu; phone, 409-772-0754; fax, 409-747-4751.
[1]Abbreviations: DSE, denatured state ensemble; TMAO, trimethylamine *N*-oxide.

 Published on Web 01/14/2010

and of the native state. Given that the DSE is the state most affected by osmolytes such as urea, sarcosine, and TMAO, it is desirable to dissect the overall energetics of osmolyte−DSE interaction and accompanying structural changes.

Urea, sarcosine, and TMAO are known to cause substantial changes in R_h and secondary structure in the DSE of proteins (*17*, *20*). Here, we take advantage of the fact that the high degree of thermal energy in thermally denatured protein favors the denatured state to the extent that substantial amounts of either the denaturing osmolyte, urea, or the protecting osmolyte, sarcosine, can be present without populating the native state significantly. This increases the experimentally accessible range for observing osmolyte-induced accretion of structure and corresponding contraction of the denatured state R_h in the absence of the native state. The protein we use, Nank 4−7*, 15 kDa, is a truncated version of the ankyrin domain of the *Drosophila* notch receptor (*16*), comprising four tandem ankyrin repeats. Nank4−7* is marginally stable at pH 7 in 200 mM NaCl, with a melting temperature of 34 °C (*14*, *16*), and at 55 °C in the presence and absence of osmolytes, the protein populates the denatured state to >99.5% under experimental conditions adopted in this study.

We use transfer free energies to assess how urea, sarcosine, and TMAO affect protein stability and the denatured ensemble (*2*, *17*, *24*). Adopting the basic approach of Nozaki and Tanford, we previously redetermined and extended their measurements by including activity coefficient data for glycine in water and 1 M urea to obtain corrected side chain transfer free energies (*3*, *25*, *26*). Contrary to Nozaki and Tanford's earlier conclusions, our published data show that urea does not denature proteins by favorable interactions with nonpolar side chains; rather it is through its favorable interactions with the peptide backbone that urea is such a good denaturant (*3*, *8*, *27*−*29*). In the present work we show that increased backbone−backbone interactions are coordinated with secondary structure accretion and contraction of the DSE that occurs upon dilution from a comparatively good solvent (urea) to the successively poorer solvents, water, sarcosine, or TMAO solution. That is, backbone−backbone interactions (intrachain hydrogen bonding) progressively increase as solvent quality is shifted from good to poor. In marked contrast, the strength of hydrophobic interactions remains relatively unchanged during this dilution process. These results permit separation of the relative roles of hydrogen-bonding and hydrophobic interactions in the DSE.

MATERIALS AND METHODS

Chemicals. NaCl was from Fisher Scientific; Na_2HPO_4 and $NaH_2PO_4 \cdot H_2O$ were obtained from Mallinckrodt. Ultapure urea was purchased from USB, sarcosine from Fluka, glycinebetaine from Sigma, and TMAO was synthesized and purified as described previously (*30*). Prior to use, all sarcosine solutions were treated with activated carbon (Aldrich) and filtered through 0.22 μm sterile filters (Millipore Millex GP), and their molar concentrations were determined refractometrically. The buffer used for all final experiments was 10 mM sodium phosphate, pH 7, and 200 mM NaCl.

Protein Expression and Purification. The C-terminal His_6-tagged Nank4−7* construct used in this study contains four tandem ankyrin repeat sequences and was expressed and purified as in refs 31 and 16.

Circular Dichroism. Temperature scans from 5 to 75 °C were performed in a Jasco J-720 spectropolarimeter at 228 nm in two

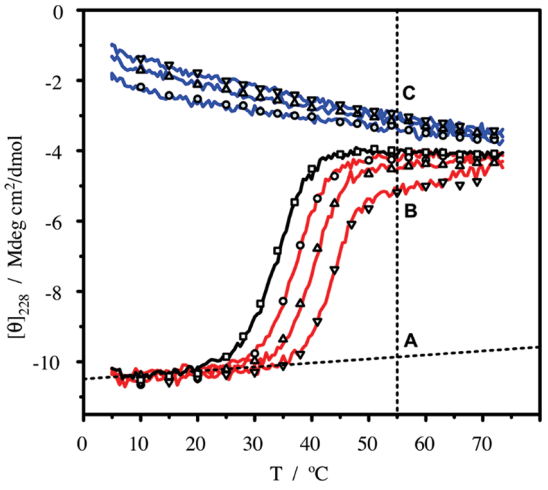

FIGURE 1: Temperature scans of Nank4−7* monitored by CD. Direct thermal scans and discrete points at 228 nm were taken to illustrate reproducibility. Thermal scans of Nank 4−7* are shown in the absence (recorded black line and open squares) and presence of sarcosine (recorded red lines) at 0.3 M (open circles), 0.6 M (open triangles), and 1 M concentrations (open inverted triangles). Also shown are thermal scans in urea (recorded blue lines) at 2 M (gray circles), 4 M (gray triangles), and 6 M (gray inverted triangles). All solutions contained 10 mM sodium phosphate buffer, pH 7.0, and 200 mM NaCl. Three conditions of interest at 55 °C, as explained in the text, are shown: (A) the extrapolated value for the native state baseline, (B) the thermally denatured state in the presence of 1 M sarcosine, and (C) the thermally denatured state in the presence of 6 M urea.

different ways. In one set of experiments continuous temperature scans were performed with a temperature slope of 1 °C/min. In another set, after jumping to a desired temperature (increments of 3−5 °C) the sample was equilibrated for 30 s, and a time course was measured for 4 min at lower temperatures (from 45 to 50 °C depending on the osmolyte concentration) and 90 s at higher temperatures to prevent aggregation, which in the slower, continuous scans was detectable at the highest temperatures in 1 M sarcosine (cf. denatured state baselines in Figure 1). Because of the strong absorbance of concentrated sarcosine and TMAO solutions in the range of ≤220 nm the ellipticity was recorded at 228 nm, where the signal is dominated by the contribution of α-helical and β-structures. Nank4−7* was present at 0.16 mg/mL, and a capped 1 mm cuvette was used.

Dynamic Light Scattering. Dynamic light scattering (DLS) experiments were performed at 55 °C with the protein at 0.32 mg/mL in the presence of 0, 2, and 4 M urea and at 15 °C in the absence of urea. All measurements were done in a DynaPro 99-D-50 MSTC 800 dynamic light scattering instrument from Protein Solutions. The refractive indices for the several samples at the proper temperature were obtained in a Milton Roy tabletop refractometer (Abbe 3L). The viscosities at the various temperatures for the solutions were obtained according to Perl et al. (*32*), and the hydrodynamic radii (R_h) obtained from DLS are all corrected for viscosity at the reported temperature.

Calculation of Transfer Free Energies. $\Delta G_{tr,N}$ is calculated from crystallographic coordinates of segments 4−7 of notch ankyrin protein in the manner described previously (*3*). Briefly, the Nank4−7* surface is interrogated with a probe the size of a water molecule to obtain the total solvent surface areas for each type of side chain and backbone. For the side chains, the areas are divided by the surface area of the fully exposed side chain to determine the number of each type of side chain exposed; the

total backbone surface area exposed is divided by a fully exposed glycine backbone for the number of exposed backbone units. The numbers of backbone units and each side chain type are multiplied by their corresponding transfer free energy, and the sum of the contributions represent $\Delta G_{tr,N}$.

RESULTS

Reversible Thermal Denaturation of Nank4−7 at Different Urea and Sarcosine Concentrations*. For optimal signal-to-noise ratio, CD of Nank4−7* was measured at 228 nm, a wavelength for which β-sheet, β-turns, and α-helices all give negative ellipticity while unordered structures are either positive or near zero (*33*). Temperature scans monitoring the mean residue ellipticity $[\Theta]_{228}$ were performed in two ways, resulting in different effective heating rates (Figure 1) as explained in Materials and Methods. The two sets of experiments show good agreement, reproducibility, and excellent reversibility. Only in the slow scan at 1 M sarcosine is evidence of protein aggregation indicated by the irregular and nonlinear behavior above 65 °C, whereas such irregularities are not seen in the temperature-jump experiments, which successfully minimize the exposure time of denatured protein at high temperatures. Urea concentration ≥2 M denatures this protein at all temperatures shown (blue lines in Figure 1). In contrast, sarcosine stabilizes the protein against temperature denaturation, increasing the transition midpoint temperature T_m (red lines in Figure 1) relative to the protein in buffer alone (black line in Figure 1). The denatured state $[\Theta]_{228}$ at temperatures ≥55 °C becomes progressively more negative on successive transfer from high urea concentration to buffer and to 1 M sarcosine. For urea-denatured protein, the decrease in $[\Theta]_{228}$ with increasing temperature is presumably due to conversion of polyproline II structure that populates the denatured ensemble at low temperature to β structure that becomes dominant at high temperature (*34*, *35*).

The CD and Volume of Nank4−7 Species Are Inversely Correlated*. In considering the specific effects of urea concentration on denatured Nank4−7*, dynamic light scattering (DLS) experiments were performed on thermally denatured Nank4−7* at 55 °C in 0, 2, and 4 M urea solutions, and R_h of the DSE was determined at each condition. R_h for thermally denatured Nank4−7* is 29.5 ± 1.0 Å in dilute buffer and 31.8 ± 1.6 Å in 2 M and 33.4 ± 1.3 Å in 4 M urea solutions, demonstrating expansion of the DSE at 55 °C as a function of urea concentration. Unfortunately, sarcosine and other protecting osmolytes give an excessively noisy DLS signal even in the absence of protein, thus preventing determination of R_h in solutions of protecting osmolytes. R_h of the protein in the presence of protecting osmolytes may be estimated from the relationship between DSE size and its CD signal. Figure 2 illustrates that the inverse of the relative hydrodynamic volume of the thermally denatured Nank4−7* species at 55 °C in the absence and presence of 2 and 4 M urea is proportional to the measured CD at 228 nm. Uversky and Fink reported such proportionality behavior at a different wavelength for intermediate states of a variety of proteins (*23*). The proportionality is observed to hold for the denatured species and native Nank4−7* as defined by

$$(R_h^{\otimes}/R_h)^3 = (1.298 \pm 0.002)([\theta]_{228}/[\theta]_{228}^{\otimes}) - (0.297 \pm 0.003) \quad (1)$$

Here, $[\theta]_{228}^{\otimes}$ and $(R_h^{\otimes})^3$ represent the ellipticity and hydrodynamic volume of Nank4−7* in buffer at 55 °C as a reference state, and

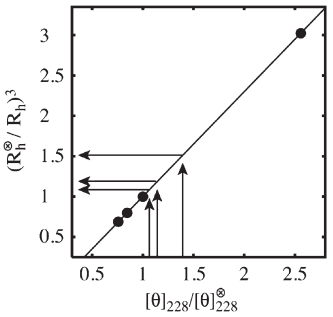

FIGURE 2: Relationship between hydrodynamic volume and CD. The hydrodynamic volume (degree of compactness) of Nank4−7* species thermally denatured at 55 °C $(R_h^{\otimes})^3$ relative to the volume of thermally denatured Nank4−7* species in 0, 2, and 4 M urea $(R_h)^3$. The ratio of these two parameters is plotted as a function of the corresponding θ_{228} for the species of interest relative to $\theta_{228}^{\otimes}$ (the ellipticity of thermally denatured Nank4−7* in 0 M urea). The linear fit is defined by eq 1 in the text. From left to right, symbols are for 4, 2, and 0 M urea for thermally denatured (55 °C) Nank4−7* with native Nank4−7* (θ_{228} and R_h determined at 15 °C) at the top right of the plot. The arrows indicate values of R_h extracted from the graph using the respective θ_{228} values recorded for 0.3, 0.6, and 1.0 M sarcosine.

$(R_h)^3$ and $[\theta]_{228}$ are the hydrodynamic volumes and corresponding ellipticities of native Nank4−7* along with thermally denatured Nank4−7* species in the absence and presence of 2 and 4 M urea concentrations. Given that DSE dimensions in the presence of sarcosine and urea are part of the same continuum of effects (*17*), Figure 2 and eq 1 were used to obtain R_h values of 34.0, 28.6, 28, and 26.8 Å, respectively, for the DSE in 6 M urea and 0.3, 0.6, and 1.0 M sarcosine solutions at 55 °C.

Contraction of Thermally Denatured Nank4−7 in Poor Solvents*. With knowledge of R_h for thermally denatured DSE at 55 °C in the presence and absence of various concentrations of urea and sarcosine, we can determine the degree to which the various solvents alter the denatured state dimensions in comparison with corresponding proteins exhibiting classical random coil behavior. Figure 3A is a composite log−log plot of R_g and R_h vs protein chain length of data from Kohn et al. and Uversky (*36*, *37*) which shows that R_g and R_h are indistinguishable for denatured states in the molecular weight range of Nank4−7*, as was also suggested previously (*22*, *23*). Figure 3B is an expansion of Figure 3A and gives the order of decreasing hydrodynamic radii of Nank4−7* species in solutions containing 4, 2, and 0 M urea and 0.3, 0.6, and 1.0 M sarcosine. The dashed lines are the 95% confidence interval for the fit of the combined R_g and R_h data. The order of decreasing R_h parallels the increasingly poorer solvent quality exhibited by these solvents. Figure 3B shows that, for all urea concentrations, R_h of Nank4−7* is below the random coil average and thermally denatured protein is on the border of the 95% confidence line. The combined information in Figures 2 and 3 illustrates that a substantial degree of structure in the DSE can be accreted while still within the 95% confidence interval of accepted random coil values, a result consistent with computational projections (*38*). In sarcosine solutions the R_h values fall outside the 95% confidence interval, and in 1 M sarcosine contraction of the thermally denatured Nank4−7* attains its most compact form without formation of a significant native state population.

Sarcosine and TMAO Are More Effective in Inducing Secondary Structure Than Urea Is at Eliminating It. Figure 4 shows how $[\Theta]_{228}$ for thermally denatured Nank4−7* changes as a function of osmolyte concentration at 61 °C. A temperature

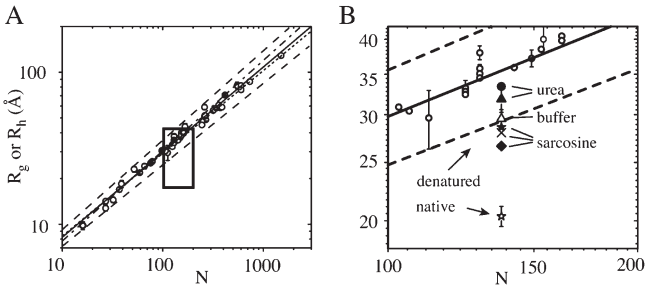

FIGURE 3: Full range of dimensional changes in Nank4−7* relative to literature values. (A) R_h and/or R_g as a function of the number of amino acids (N) in the protein. The solid line is a fit through all of the data with the 95% confidence limits (heavy dashed lines). The dot-dashed line is a fit through the R_g data from Kohn et al. (*36*) and the light dotted line a fit through the R_h data from Uversky (*37*). The open square in the plot represents the region expanded for panel B. (B) R_h values for Nank4−7* are reported in the context of a plot of R_h (*37*) and R_g (*36*) values as a function of protein chain length. R_h values reported for Nank4−7* species in 0.3, 0.6, and 1 M sarcosine solutions were calculated from their measured θ_{228} values using eq 1. Key: filled circle, 4 M urea (33.4 Å); filled triangle, 2 M urea (31.8 Å); open triangle, thermally denatured state (29.5 Å); filled star, 0.3 M sarcosine (28.6 Å); cross, 0.6 M sarcosine (28.0 Å); filled diamond, 1 M sarcosine (26.6 Å); open star, native Nank4−7*.

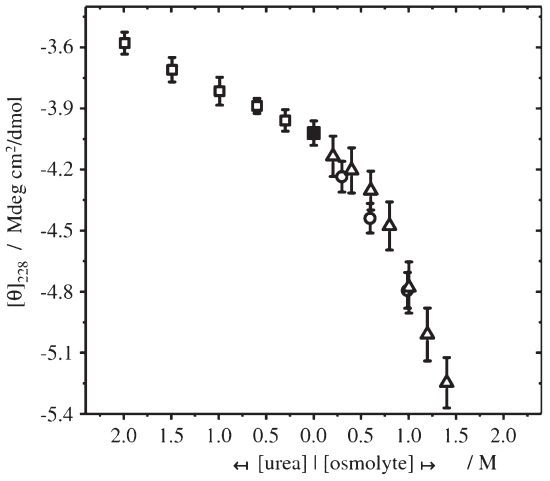

FIGURE 4: Molar ellipticity for the Nank 4−7* denatured state at 61 °C in 10 mM sodium phosphate, pH 7.0, and 200 mM NaCl as a function of cosolvent concentration. Molar ellipticity at 228 nm is given as a function of urea and several protecting osmolyte concentrations including urea (open squares), sarcosine (circles), and TMAO (triangles). Nank 4−7* in the absence of the osmolytes is represented as a closed square.

higher than 55 °C was used so that higher osmolyte concentration could be employed while still not populating the native state. Clearly, urea is not as effective in reducing secondary structure in thermally denatured Nank4−7* as sarcosine and TMAO are at inducing such structure. It is known that TMAO is frequently more effective in folding proteins than urea is in unfolding them (*16*, *39*), and this is attributed largely to the fact that urea's interaction free energy with the peptide backbone is opposite in sign and much smaller in magnitude than that of TMAO and sarcosine (*14*, *40*). It should be noted in Figure 4 that sarcosine and TMAO are equally effective at inducing secondary structure into thermally denatured Nank4−7*.

Structural Energetics of a DSE under Folding Conditions. Figures 1−4 provide evidence of significant effects of urea, sarcosine, and TMAO on secondary structure content of thermally denatured Nank4−7* that is coordinated in a well-defined manner with the hydrodynamic volume. The experiments explore how the structure of a DSE responds to changes in solvent quality induced by physiologically important osmolytes at a temperature in which the denatured state is >99% populated. The same types of tendencies exhibited at high temperature also occur at temperatures in which folding/unfolding occurs, and this lower temperature range, that is of interest in protein folding, is the focus of the remainder of the Results section.

Table 1: Nank4−7* Transfer Free Energies and *m*-Values[a]

	$\Delta G_{tr,D}$		$\Delta G_{tr,N}$		$\Delta\Delta G_{tr}$		*m*-value (kcal mol^{-1} M^{-1})	
osmolyte	sc	bb	sc	bb	sc	bb	predicted	exptl
urea	0.87	−3.05	0.55	−1.09	0.32	−1.96	−1.64	−1.9 ± 0.1
sarcosine	−0.26	4.07	−0.44	1.45	0.18	2.62	2.8	2.8 ± 0.2
TMAO	−2.60	7.04	−1.34	2.50	−1.26	4.54	3.28	nd

[a]Transfer free energies (kcal/mol) for the denatured (D) and native (N) states from water to 1 M concentrations of either sarcosine or urea. For illustration, the transfer free energies for N or D states are dissected into contributions from side chains (sc) and backbone (bb). The *m*-value for sarcosine or urea ($\Delta\Delta G_{tr}$) is given by $\Delta G_{tr,D} - \Delta G_{tr,N}$ as described in Auton and Bolen (*2*). Sarcosine and urea experimental *m*-values for Nank4−7* were taken from Holthauzen and Bolen (*14*).

Folding Cooperativity of Nank 4−7 in Urea and Sarcosine Solutions Is Dominated by Backbone Contributions*. The *m*-value, an experimental thermodynamic quantity determined by use of the linear extrapolation method, measures the cooperativity of protein folding/unfolding induced by an osmolyte (*41*). It is evaluated as the slope of the linear plot of protein stability vs osmolyte concentration, and it represents the water to 1 M osmolyte transfer free energy contributed by those side chain and backbone groups that become newly exposed upon denaturation by urea or newly buried on being forced to fold by protecting osmolytes (*2*, *3*, *24*). Using transfer free energies and the Tanford transfer model, we recently demonstrated the ability to predict *m*-values of proteins successfully (*2*, *3*). The method accounts for transfer free energies of the native ($\Delta G_{tr,N}$) and denatured states ($\Delta G_{tr,D}$) by summing individual side chain and backbone contributions (Δg_{tr}) (*2*, *24*, *42*). The free energy difference ($\Delta G_{tr,D} - \Delta G_{tr,N}$ = *m*-value) is then used to quantify residue-level free energy contributions of those groups that contribute to the *m*-value (*2*, *3*, *24*). For Nank 4−7*, Table 1 lists the collective free energy contributions of side chains and of backbone upon transfer of the native and denatured states from water to 1 M urea or sarcosine. The model used for the denatured state is a self-avoiding random coil (*2*, *24*, *43*). Determined in this way, *m*-values of opposite sign are obtained for denaturants and stabilizers, respectively, and the calculated and experimentally determined *m*-values are found to be in good agreement (Table 1).

It is clear from Table 1 that the side chains collectively contribute very little (0.18 and 0.32 kcal/mol) to the sarcosine and urea effects on protein stability; the major contribution comes from the backbone (2.62 and −1.96 kcal/mol). With urea, the large favorable backbone transfer promotes denaturation and overcomes a small resistance to unfolding (positive sign) collectively from the side chains; conversely, with sarcosine the large unfavorable interaction with backbone promotes folding while side chains collectively contribute little.

Urea Is a Good Solvent for the Peptide Backbone but Not for Side Chains. For transfer of Nank4−7* DSE from water to 1 M urea, Figure 5A gives a residue-level accounting of the

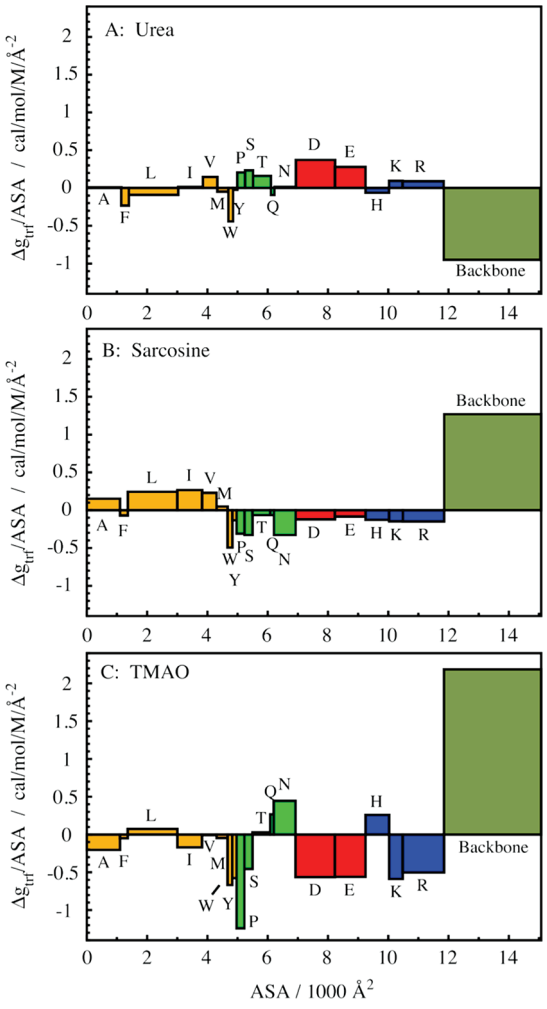

FIGURE 5: Side chain and backbone contributions to $\Delta G_{tr,D}$ of Nank4−7* DSE from water to 1 M urea (A), sarcosine (B), and TMAO (C) solution. Side chain and backbone transfer free energy contributions (Δg_{tr}) divided by the corresponding surface areas exposed in the DSE are plotted as a function of those solvent-exposed surface areas. Backbone contributions are represented by the color dark green, whereas basic, acidic, polar, and nonpolar side chains are in blue, red, green, and yellow, respectively, and standard letters identify the side chains. The area under each bar is proportional to the transfer free energy contribution of that AA side chain to $\Delta G_{tr,D}$. The denatured state model used is a self-avoiding random coil with side chain and backbone surface areas evaluated as described previously (*3*). Numerical values for side chains and backbone contributions are given in Table 2.

contributions to the denatured state transfer free energy. The abscissa gives the surface area of the groups exposed in Nank4−7* DSE using a self-avoiding random coil as a model (*3*). The ordinate is the group free energy contribution per square angstrom, with the corresponding areas representing the free energy contribution to $\Delta G_{tr,D}$ of that type of group. The algebraic sum of all contributions equals $\Delta G_{tr,D}$. It is clear from Figure 5A that the favorable interaction of peptide units with urea dominates the DSE transfer free energy and that the collective contribution of side chains is small and unfavorable (see Table 1). It is also clear from Table 2 that nonpolar groups contribute both favorably and unfavorably to the transfer, with the sum being favorable in this case, amounting to ~10% of the total denatured state transfer free energy. This means that the strength of hydrophobic interactions in this protein is relatively unchanged on transfer from water to urea solution.

Table 2: Side Chain and Backbone Contributions to $\Delta G_{tr,D}$

	$\Delta G_{tr,D}$(cal/mol)						
osmolyte	nonpolar	polar	acidic	basic	$\sum$sc	bb	total
urea	−210	206	765	114	875	−3053	2178
sarcosine	799	−449	−244	−370	−264	4071	3807
TMAO	−520	−75	−1308	−753	−2598	7046	4448

While the *m*-value gives the free energy dependence of folding/unfolding on osmolyte type and concentration, the transfer free energy of the denatured state ($\Delta G_{tr,D}$) provides the driving force responsible for the physical and spectral changes the DSE undergoes in response to osmolyte type and concentration as shown in Figures 2−4. The breakdown of $\Delta G_{tr,D}$ in Table 1 shows that transfer of the DSE from water to 1 M urea is favorable (0.87 − 3.05 = −2.18 kcal/mol). For the sake of illustration, DSE transfer to 6 M urea, as in the case of Nank4−7*, is highly favorable ($C_{urea}\Delta G_{tr,D}$ = −13.1 kcal/mol), and this net favorable transfer free energy is composed of a −18 kcal/mol contribution from the favorable interaction of 6 M urea with the DSE peptide backbone and a (0.32 × 6 = 1.92 kcal/mol) unfavorable interaction of the urea with those groups destined to be buried on folding, along with 3.3 kcal/mol unfavorable urea interaction with the solvent-exposed side chains of the native protein. Based on these transfer free energies, it can be concluded that 6 M urea is a good solvent for the peptide backbone but not for the side chains. The magnitude of the favorable interaction of urea with peptide backbone is sufficient to drive DSE structural and spectral changes as shown in Figures 1, 2, and 3B.

TMAO and Sarcosine Are Poor Solvents for the Peptide Backbone with Side Chains Contributing Differentially but Marginally Overall to the DSE Transfer Free Energy. Figure 5 shows residue-level free energy contributions upon transfer of the denatured state from water to 1 M sarcosine (Figure 5B) and from water to 1 M TMAO (Figure 5C), and with both protecting osmolytes the unfavorable interaction with peptide backbone dominates the DSE transfer free energy. Clearly, sarcosine and TMAO are poor solvents for the peptide backbone. It is interesting to note that for transfer to sarcosine the side chains collectively contribute very little to the DSE transfer free energy (as reflected in Table 1). This is because the unfavorable interaction with the hydrophobic class of side chains is offset by the favorable interaction between sarcosine and the polar and charged side chain classes of residues. In contrast to sarcosine, the hydrophobic side chains collectively interact favorably with TMAO as do the polar and charged side chains, leading to an overall favorable TMAO interaction with side chains that is opposed by a very large unfavorable and dominant TMAO interaction with backbone. Whereas both TMAO and sarcosine have the same general effects on the dimensions and structural accretion of the Nank4−7* DSE (see ref 17 and Figure 4), the differences in their interactions with side chains (Figure 5 and Table 2) serve to illustrate important distinctions between TMAO and sarcosine.

DISCUSSION

*Osmolytes Induce Large Changes in the Hydrodynamic Volume and Secondary Structure of Thermally Denatured Nank4−7**. Transfer of (55 °C) thermally denatured Nank4−7* in 6 M urea to progressively poorer solvents, water and then sarcosine or TMAO solutions, causes large reduction in R_h of the

DSE with concomitant accretion of secondary structure. Specifically, the DSE contracts (Figures 2 and 3B) such that in 1 M sarcosine its volume ratio is about twice that of native Nank4−7*, a highly compact ensemble approximating the relative size expected of a premolten globule state (*44*). Moreover, the magnitude of structure accretion (C to B in Figure 1) accompanying this contraction is itself substantial, amounting to ~30% of the total CD change possible on going from the protein denatured in 6 M urea to the fully folded state (C to A in Figure 1) at this temperature.

What kind of structure is accumulated upon Nank4−7* contraction? While the ellipticities of unstructured polypeptide structures at Θ_{228} are positive or close to zero, β-sheet, β-turns, and α-helices are all negative at this wavelength (*33*). Intrachain hydrogen bonding defines backbone−backbone interactions, and the low contact order α-helix and β-hairpin structures are likely to be populated because they are particularly effective at reducing exposure of the peptide backbone to sarcosine or TMAO, thus mitigating the positive free energy of the DSE upon transfer of the peptide backbone to these poor solvents. Relative to water, osmolytes like sarcosine and TMAO increase helical content in peptides that have helix-forming propensity (*45*). Nank4−7* has ample α-helix and β-hairpin propensities, given that the native protein is 46% helical and contains several β-hairpins (*46*). Indeed, the type of interactions responsible for decreasing R_h (through intrachain hydrogen bonds) is also the one responsible for secondary structure, resulting in the accretion of secondary structure and contraction of the denatured ensemble being interrelated processes (Figure 2).

These results illustrate that under the equilibrium conditions presented the DSE can accommodate dimensional and structure accretion changes from a random coil to a premolten globule without substantively populating the native state. Such behavior provides strong support for the hierarchical model of protein folding under equilibrium conditions, and the high population of the DSE species enables investigations of the nature of accreted structure in the DSE and the extent to which it is native-like.

There is ample evidence that structural and dimensional changes we observed with the DSE at high temperature also occur around room temperature, where most protein folding studies have been performed. The osmolyte urea is known to expand, and osmolytes like TMAO and sarcosine contract the R_h of the DSE at 25 °C (*17*) and at 55 °C shown here. Contraction and structure accretion are interrelated by $(R_h)^{-3}$ being directly proportional to [Θ] as shown by Uversky and Fink in the range of room temperature and at 55 °C shown here. What is missing is the relationship between the free energy of the DSE and the DSE's structural and dimensional changes as solvent quality is changed. Such information is available at 25 °C from transfer free energy measurements (*17*), thus allowing a structural energetic interpretation of the solvent-induced DSE contraction and structural accretion frequently observed at room temperature.

*Structural Energetics of Osmolyte-Mediated Changes in the DSE of Nank4−7**. The sign of the transfer free energy for a denatured protein provides the basis for concepts such as solvophilicity, solvophobicity, and solvent quality (*1*, *24*, *47*). The sign and magnitude of the transfer free energy for the entire denatured state ($\Delta G_{tr,D}$), obtained by summing the transfer free energy contributions of all its constituent groups, determine the overall solvent quality experienced by the polymer chain (*1*, *17*, *47*). Key to discussions of hydrophobic interactions and hydrogen bonding are the striking parallels in how these forces

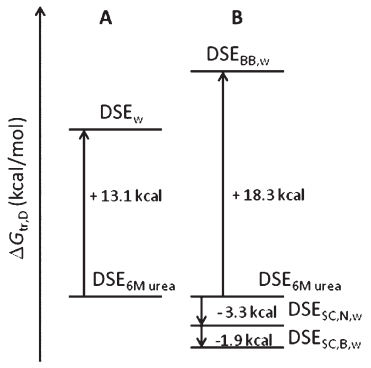

FIGURE 6: Nank4−7* DSE transfer free energy from 6 M urea (DSE_{6Murea}) to water (DSE_w). The left side shows the net transfer free energy change. The right side represents group contributions to the net free energy from transfer of the backbone to water ($DSE_{bb,w}$), along with transfer of those side chains destined for burial on protein folding ($DSE_{sc,B,w}$) and side chains that are solvent exposed in the native state ($DSE_{sc,N,w}$).

are mediated by water and protecting osmolytes and in how they effect protein folding and changes in the DSE. On the basis of the positive free energy of transfer (Δg_{tr}) of nonpolar groups from a nonpolar solvent to water, water is said to be a poor solvent for nonpolar groups (*48*−*50*). Upon transfer to water the hydrodynamic radius of a DSE that contains nonpolar residues contracts in a process referred to as hydrophobic collapse (*51*). The DSE collapses because monomer−monomer contacts (nonpolar side chain−nonpolar side chain, i.e., hydrophobic interactions) are more favorable than monomer−solvent contacts (*50*, *52*−*54*).

As with hydrophobic collapse, protecting osmolyte solvents such as sarcosine and TMAO solutions also are quite effective at causing contraction of the DSE, but a different part of the protein structure is responsible, namely, the peptide backbone (*17*). Δg_{tr} of the peptide backbone from water to either TMAO or sarcosine solution is positive and depends monotonically on osmolyte concentration, thus classifying sarcosine and TMAO as poor solvents for the peptide backbone (*14*, *47*, *55*−*57*). Upon transfer of the denatured state from water to sarcosine or TMAO solution, monomer−monomer contacts (backbone−backbone, i.e., intrachain hydrogen-bonding interactions) of the DSE are more favorable than backbone−sarcosine/TMAO contacts, thus causing DSE contraction and accretion of secondary structure (*17*, *45*) in what is known as the osmophobic effect (*6*). In both instances, the impetus for DSE contraction is the respective positive free energy of transfer, with nonpolar interactions favored over the interactions between the nonpolar group and water in the case of hydrophobic collapse and with intrachain hydrogen-bonding interactions favored over the interactions between peptide backbone units and sarcosine or TMAO solution in the case of osmophobic collapse. In essence, both hydrophobic interactions and hydrogen bonding owe their magnitudes to solvent quality.

DSE Contraction and Secondary Structure Accretion Are Driven by the Free Energy Increase on DSE Transfer to Successively Poorer Solvents, Water and Sarcosine. To understand how the driving force for DSE structural and spectral changes arises from denatured state transfer free energies ($\Delta G_{tr,D}$), it is useful to focus on the details of free energy contributions to the transfer. Table 1 shows that Nank4−7* DSE transfer from 1 M urea to water at 25 °C, $\Delta G_{tr,D}$, is 2.18 kcal mol^{-1} M^{-1}, and the net transfer from 6 M urea to water is 6-fold larger, 13.1 kcal/mol (Figure 6A). The DSE will respond

to this large unfavorable free energy in ways to reduce contact between thte peptide backbone and water. Depending on conditions this may include transition to the native state, DSE aggregation, or DSE contraction (*47*).

Figure 6B shows how this large net unfavorable free energy upon transfer of the DSE from 6 M urea to water is parsed into backbone and side chain contributions. First, ($6 \times 3.0 \cong$ 18.3 kcal/mol) in free energy change occurs on transfer to the DSE peptide backbone, showing that in comparison to 6 M urea water is a poor solvent for the peptide backbone. Thus, a strong relative increase in intrachain hydrogen bonding occurs on DSE transfer as urea−backbone interactions decline to zero, and this drives contraction of R_h and accretion of structure. At the same time, the side chains *collectively* favor transfer to water ($6 \times (-0.875) \cong -5.3$ kcal/mol), tending to cause some R_h expansion of the DSE, but this is overridden by the +18.3 kcal/mol effect on the backbone (see Table 2 and Figure 5A). As a class, the DSE's nonpolar groups favor the transfer to water ($6 \times (-0.21) \cong -1.26$ kcal/mol) (Table 2), but as also shown by others the effect is quite small (*58*), particularly in comparison with transfer of the peptide backbone.

In summary, we emphasize that the strength of hydrophobic interactions is not altered substantively by the presence of urea. Indeed, small clusters of hydrophobic groups have been observed in the DSEs, even in high urea concentration. By contrast, urea significantly affects hydrogen-bonding interactions in the DSE. Urea interacts favorably with the peptide backbone through direct H-bonding (*12*), which causes disruption of hydrogen-bonded secondary structure and expansion of the polymer chain. Denaturation occurs at urea concentrations in which the favorable urea−backbone interactions that promote the DSE exceed the strength of those intramolecular interactions that maintain the integrity of the native state. Thermodynamically, these processes are reversed on dilution of urea-denatured protein to native conditions.

Hydrophobic Interactions in Osmolyte Solutions. For decades hydrophobic interactions have been considered the driving force for DSE contraction on transfer from urea solution to water (*50*, *59*). However, from a polymer science perspective Figures 5 and 6 show that the free energy of intrachain hydrogen-bonding interactions changes considerably more than hydrophobic interactions upon DSE transfer from urea to water. This is not to say that hydrophobic interactions play no role in the DSE contraction and ultimate transition to the native state. Indeed, hydrophobic interactions remain strong even in 8 M urea solution. Our view is that while hydrophobic interaction free energy remains approximately the same in urea and in water, the reduction in DSE R_h resulting from the increased intrachain hydrogen bonding upon diluting the urea ultimately increases the local concentration of hydrophobic side chains. This leads to increased nonpolar group proximity, and hydrophobic interactions increasingly engage. With further urea dilution the reduced urea−backbone interactions continue to decline until they are unable to rival the strength of all the intramolecular interactions involved in maintaining the integrity of the native state, and at this point the native state populates to a measurable degree.

The free energy effects of sarcosine and TMAO on Nank4−7* DSE structure and dimensions provide interesting contrasts to that of urea. First, the large unfavorable interaction between these osmolytes and the peptide backbone (see Figure 5B,C) is responsible for the large positive $\Delta G_{tr,D}$ which is ameliorated by reducing contact of the backbone with solvent through contraction of the R_h concomitant with accretion of secondary structure. Table 2 shows that for both protecting osmolytes the side chains collectively oppose the large unfavorable interaction of osmolyte with backbone. However, a major important difference between the two protecting osmolytes can be found in how the nonpolar groups respond to the transfer. Panels B and C of Figure 5 show that the nonpolar groups interact unfavorably with sarcosine while interacting favorably with TMAO. That is, in TMAO solution secondary structure accretion, DSE contraction, and protein folding are driven by the unfavorable interaction with the peptide backbone, and these processes are opposed to a small extent by hydrophobic interactions. In the presence of sarcosine, DSE contraction, structure accretion, and protein folding again are driven by the unfavorable interaction with the peptide backbone, but in this case hydrophobic interactions favor contraction and folding. These differences between osmolytes can potentially be used in further differentiation of hydrophobic and osmophobic effects within DSEs (*6*).

Intrinsically disordered proteins provide an opportunity to examine further the roles of hydrophobic groups and backbone in contracting the DSE and folding the protein. These proteins are disordered in aqueous solution and are significantly depleted in bulky nonpolar and aromatic side chains (*60*), and those whose sequence contains folding information can be forced to fold if solvent quality is made poor enough. Addition of TMAO or sarcosine to examples of such intrinsically disordered proteins causes contraction of the DSE and cooperative folding to species that have structure and function (*15*, *61*−*63*). For a DSE the size of Nank4−7*, Table 1 provides data from which it can be shown that a 6 M TMAO solution raises the backbone free energy by 42 kcal/mol and that whatever nonpolar groups are present should oppose folding to a modest degree. TMAO solution is clearly a much poorer solvent for the backbone than water, and the large unfavorable free energy of the peptide backbone is reduced through contraction/secondary structure accretion of the DSE and particularly from burial of the backbone through folding. The fact that such proteins have low hydrophobicity indices emphasizes the key role of hydrogen bonding and backbone burial in TMAO-induced folding of IDPs.

ACKNOWLEDGMENT

Early in this work, Doug Barrick was most helpful in discussions and providing the expression system for Nank4−7*, which we gratefully acknowledge. We also thank Matthew Auton for preparing some figures and George Rose for contributions in discussions throughout the work and in editing the manuscript.

REFERENCES

1. Bolen, D. W., and Rose, G. D. (2008) Structure and energetics of the hydrogen-bonded backbone in protein folding. *Annu. Rev. Biochem. 77*, 339–362.
2. Auton, M., and Bolen, D. W. (2005) Predicting the energetics of osmolyte-induced protein folding/unfolding. *Proc. Natl. Acad. Sci. U.S.A. 102*, 15065–15068.
3. Auton, M., Holthauzen, L. M., and Bolen, D. W. (2007) Anatomy of energetic changes accompanying urea-induced protein denaturation. *Proc. Natl. Acad. Sci. U.S.A. 104*, 15317–15322.
4. Hochachka, P. W., and Somero, G. N. (2002) Biochemical Adaptation. Mechanism and Process in Physiological Evolution, Oxford University Press, Oxford.
5. Yancey, P. H., Clark, M. E., Hand, S. C., Bowlus, R. D., and Somero, G. N. (1982) Living with water stress: evolution of osmolyte systems. *Science 217*, 1214–1222.

6. Bolen, D. W., and Baskakov, I. V. (2001) The osmophobic effect: natural selection of a thermodynamic force in protein folding. *J. Mol. Biol. 310*, 955–963.
7. Timasheff, S. N. (1993) The control of protein stability and association by weak interactions with water: how do solvents affect these processes? *Annu. Rev. Biophys. Biomol. Struct. 22*, 67–97.
8. Courtenay, E. S., Capp, M. W., Saecker, R. M., and Record, M. T., Jr. (2000) Thermodynamic analysis of interactions between denaturants and protein surface exposed on unfolding: interpretation of urea and guanidinium chloride m-values and their correlation with changes in accessible surface area (ASA) using preferential interaction coefficients and the local-bulk domain model. *Proteins, Suppl. 4*, 72–85.
9. Davis-Searles, P. R., Saunders, A. J., Erie, D. A., Winzor, D. J., and Pielak, G. J. (2001) Interpreting the effects of small uncharged solutes on protein-folding equilibria. *Annu. Rev. Biophys. Biomol. Struct. 30*, 271–306.
10. Schellman, J. A. (2002) Fifty years of solvent denaturation. *Biophys. Chem. 96*, 91–101.
11. Zou, Q., Bennion, B. J., Daggett, V., and Murphy, K. P. (2002) The molecular mechanism of stabilization of proteins by TMAO and its ability to counteract the effects of urea. *J. Am. Chem. Soc. 124*, 1192–202.
12. Lim, W. K., Rösgen, J., and Englander, S. W. (2009) Urea, but not guanidinium, destabilizes proteins by forming hydrogen bonds to the peptide group. *Proc. Natl. Acad. Sci. U.S.A. 106*, 2595–2600.
13. Baskakov, I., and Bolen, D. W. (1998) Forcing thermodynamically unfolded proteins to fold. *J. Biol. Chem. 273*, 4831–4834.
14. Holthauzen, L. M., and Bolen, D. W. (2007) Mixed osmolytes: The degree to which one osmolyte affects the protein stabilizing ability of another. *Protein Sci. 16*, 293–298.
15. Henkels, C. H., Kurz, J. C., Fierke, C. A., and Oas, T. G. (2001) Linked folding and anion binding of the *Bacillus subtilis* ribonuclease P protein. *Biochemistry 40*, 2777–2789.
16. Mello, C. C., and Barrick, D. (2003) Measuring the stability of partly folded proteins using TMAO. *Protein Sci. 12*, 1522–1529.
17. Qu, Y., Bolen, C. L., and Bolen, D. W. (1998) Osmolyte-driven contraction of a random coil protein. *Proc. Natl. Acad. Sci. U.S.A. 95*, 9268–9273.
18. Möglich, A., Joder, K., and Kiefhaber, T. (2006) End-to-end distance distributions and intrachain diffusion constants in unfolded polypeptide chains indicate intramolecular hydrogen bond formation. *Proc. Natl. Acad. Sci. U.S.A. 103*, 12394–12399.
19. Rose, G. D., Fleming, P. J., Banavar, J. R., and Maritan, A. (2006) A backbone-based theory of protein folding. *Proc. Natl. Acad. Sci. U.S.A. 103*, 16623–16633.
20. Sosnick, T. R., Shtilerman, M. D., Mayne, L., and Englander, S. W. (1997) Ultrafast signals in protein folding and the polypeptide contracted state. *Proc. Natl. Acad. Sci. U.S.A. 94*, 8545–8550.
21. Tran, H. T., Mao, A., and Pappu, R. V. (2008) Role of backbone-solvent interactions in determining conformational equilibria of intrinsically disordered proteins. *J. Am. Chem. Soc. 130*, 7380–7392.
22. Ziv, G., Thirumalai, D., and Haran, G. (2009) Collapse transition in proteins. *Phys. Chem. Chem. Phys. 11*, 83–93.
23. Uversky, V. N., and Fink, A. L. (2002) The chicken-egg scenario of protein folding revisited. *FEBS Lett. 515*, 79–83.
24. Auton, M., and Bolen, D. W. (2007) Application of the transfer model to understand how naturally occurring osmolytes affect protein stability. *Methods Enzymol. 428*, 397–418.
25. Nozaki, Y., and Tanford, C. (1963) The solubility of amino acids and related compounds in aqueous urea solutions. *J. Biol. Chem. 238*, 4074–4081.
26. Rafflenbeul, L., Pang, W.-M., Schönert, H., and Haberle, K. (1973) Zur thermodynamik der hydrophoben wechselwirkung; die systeme wasser+glycin+harnstoff und wasser+alanin+harnstoff bei 25 C. *Z. Naturforsch. 28*, 533–554.
27. Makhatadze, G. I., and Privalov, P. L. (1992) Protein interactions with urea and guanidinium chloride. A calorimetric study. *J. Mol. Biol. 226*, 491–505.
28. Robinson, D. R., and Jencks, W. P. (1965) The effect of compounds of the urea-guanidinium class on the activity coefficient of acetyltetraglycine ethyl ester and related compounds. *J. Am. Chem. Soc. 87*, 2462–2470.
29. Scholtz, J. M., Barrick, D., York, E. J., Stewart, J. M., and Baldwin, R. L. (1995) Urea unfolding of peptide helices as a model for interpreting protein unfolding. *Proc. Natl. Acad. Sci. U.S.A. 92*, 185–189.
30. Russo, A. T., Rösgen, J., and Bolen, D. W. (2003) Osmolyte effects on kinetics of FKBP12 C22A folding coupled with prolyl isomerization. *J. Mol. Biol. 330*, 851–866.
31. Zweifel, M. E., and Barrick, D. (2001) Studies of the ankyrin repeats of the *Drosophila melanogaster* Notch receptor. 1. Solution conformational and hydrodynamic properties. *Biochemistry 40*, 14344–14356.
32. Perl, D., Jacob, M., Bano, M., Stupak, M., Antalik, M., and Schmid, F. X. (2002) Thermodynamics of a diffusional protein folding reaction. *Biophys. Chem. 96*, 173–190.
33. Berova, N., Nakanishi, K., and Woody, R. W. (2000) Circular dichroism: principles and applications, 2nd ed., Wiley-VCH, New York.
34. Shi, Z., Olson, C. A., Rose, G. D., Baldwin, R. L., and Kallenbach, N. R. (2002) Polyproline II structure in a sequence of seven alanine residues. *Proc. Natl. Acad. Sci. U.S.A. 99*, 9190–9195.
35. Yang, W. Y., Larios, E., and Gruebele, M. (2003) On the extended beta-conformation propensity of polypeptides at high temperature. *J. Am. Chem. Soc. 125*, 16220–16227.
36. Kohn, J. E., Millett, I. S., Jacob, J., Zagrovic, B., Dillon, T. M., Cingel, N., Dothager, R. S., Seifert, S., Thiyagarajan, P., Sosnick, T. R., Hasan, M. Z., Pande, V. S., Ruczinski, I., Doniach, S., and Plaxco, K. W. (2004) Random-coil behavior and the dimensions of chemically unfolded proteins. *Proc. Natl. Acad. Sci. U.S.A. 101*, 12491–12496.
37. Uversky, V. N. (1993) Use of fast protein size-exclusion liquid chromatography to study the unfolding of proteins which denature through the molten globule. *Biochemistry 32*, 13288–13298.
38. Fitzkee, N. C., and Rose, G. D. (2004) Reassessing random-coil statistics in unfolded proteins. *Proc. Natl. Acad. Sci. U.S.A. 101*, 12497–12502.
39. Pradeep, L., and Udgaonkar, J. B. (2004) Osmolytes induce structure in an early intermediate on the folding pathway of barstar. *J. Biol. Chem. 279*, 40303–40313.
40. Wang, A., and Bolen, D. (1997) A naturally occurring protective system in urea-rich cells: mechanism of osmolyte protection of proteins against urea denaturation. *Biochemistry 36*, 9101–9108.
41. Greene, R. F., Jr., and Pace, C. N. (1974) Urea and guanidine hydrochloride denaturation of ribonuclease, lysozyme, alpha-chymotrypsin, and beta-lactoglobulin. *J. Biol. Chem. 249*, 5388–5393.
42. Tanford, C. (1964) Isothermal unfolding of globular proteins in aqueous urea solutions. *J. Am. Chem. Soc. 86*, 2050–2059.
43. Goldenberg, D. P. (2003) Computational simulation of the statistical properties of unfolded proteins. *J. Mol. Biol. 326*, 1615–33.
44. Uversky, V. N. (2002) Natively unfolded proteins: a point where biology waits for physics. *Protein Sci. 11*, 739–756.
45. Celinski, S. A., and Scholtz, J. M. (2002) Osmolyte effects on helix formation in peptides and the stability of coiled-coils. *Protein Sci. 11*, 2048–2051.
46. Sedgwick, S. G., and Smerdon, S. J. (1999) The ankyrin repeat: a diversity of interactions on a common structural framework. *Trends Biochem. Sci. 24*, 311–316.
47. Bolen, D. W. (2004) Effects of naturally occurring osmolytes on protein stability and solubility: issues important in protein crystallization. *Methods 34*, 312–322.
48. Frank, H. S., and Evans, M. W. (1945) Free volume and entropy in condensed systems. III. Entropy in binary liquid mixtures; partial molal entropy in dilute solutions; structure and thermodynamics in aqueous electrolytes. *J. Chem. Phys. 13*, 507–532.
49. Kauzmann, W. (1959) Some factors in the interpretation of protein denaturation. *Adv. Protein Chem. 14*, 1–63.
50. Dill, K. A. (1990) Dominant forces in protein folding. *Biochemistry 29*, 7133–7155.
51. Dill, K. A. (1985) Theory for the folding and stability of globular proteins. *Biochemistry 24*, 1501–1509.
52. Sanchez, I. C. (1979) Phase-transition behavior of the isolated polymer-chain. *Macromolecules 12*, 980–988.
53. deGennes, P. G. (1975) Collapse of a polymer-chain in poor solvents. *J. Phys. Lett.* (*Paris*) *36*, L55–L57.
54. Post, C. B., and Zimm, B. H. (1979) Internal condensation of a single DNA molecule. *Biopolymers 18*, 1487–1501.
55. Liu, Y., and Bolen, D. (1995) The peptide backbone plays a dominant role in protein stabilization by naturally occurring osmolytes. *Biochemistry 34*, 12884–12891.
56. Auton, M., and Bolen, D. W. (2004) Additive transfer free energies of the peptide backbone unit that are independent of the model compound and the choice of concentration scale. *Biochemistry 43*, 1329–1342.
57. Wu, P., and Bolen, D. W. (2006) Osmolyte-induced protein folding free energy changes. *Proteins 63*, 290–296.
58. O'Brien, E. P., Dima, R. I., Brooks, B., and Thirumalai, D. (2007) Interactions between hydrophobic and ionic solutes in aqueous guanidinium chloride and urea solutions: lessons for protein denaturation mechanism. *J. Am. Chem. Soc. 129*, 7346–7353.

59. Baldwin, R. L. (1989) How does protein folding get started? *Trends Biochem. Sci. 14*, 291–294.
60. Uversky, V. N., Oldfield, C. J., and Dunker, A. K. (2008) Intrinsically disordered proteins in human diseases: introducing the D2 concept. *Annu. Rev. Biophys. 37*, 215–246.
61. Baskakov, I. V., Kumar, R., Srinivasan, G., Ji, Y. S., Bolen, D. W., and Thompson, E. B. (1999) Trimethylamine N-oxide-induced cooperative folding of an intrinsically unfolded transcription-activating fragment of human glucocorticoid receptor. *J. Biol. Chem. 274*, 10693–10696.
62. Kumar, R., Baskakov, I. V., Srinivasan, G., Bolen, D. W., Lee, J. C., and Thompson, E. B. (1999) Interdomain signaling in a two-domain fragment of the human glucocorticoid receptor. *J. Biol. Chem. 274*, 24737–24741.
63. Uversky, V. N., Li, J., and Fink, A. L. (2001) Trimethylamine-N-oxide-induced folding of alpha-synuclein. *FEBS Lett. 509*, 31–35.